Original article

Institution of MECHANICAL ENGINEERS

Journal of MATERIALS: DESIGN AND APPLICATIONS

Proc IMechE Part L:
J Materials: Design and Applications
2016, Vol. 230(6) 985–993

DOI: 10.1177/1464420715591859
pil.sagepub.com

SAGE

Preparation and characterization of porous hydroxyapatite pellets: Effects of calcination and sintering on the porous structure and mechanical properties

Onder Albayrak[1], Mehmet Ipekoglu[2], Nazim Mahmutyazicioglu[3], Mehmet Varmis[1], Emrah Kaya[1] and Sabri Altintas[4]

Abstract

In this study, porous hydroxyapatite structures were produced by using urea particles of 600–850 μm size. Samples with two different urea composition (25 and 50 wt%) were prepared along with samples without any urea content by adding urea to commercially available hydroxyapatite in its as purchased and calcined states. The produced pellets were sintered at 1100 °C and 1200 °C for 2 h. Compression tests and microhardness measurements were conducted and changes in density values were examined in order to determine the effect of the calcination state of the prior hydroxyapatite powder, the sintering temperature and the amount of urea added. Also X-ray diffraction, Fourier transform infrared, and scanning electron microscopy analyses were conducted to determine the phase stability, functional groups, and pore morphology, respectively. Calcination is found to negatively affect the densification and sinterability of the produced samples, resulting in a decrease of compressive strength and microhardness. With the control of the urea content and sintering temperature uncalcined hydroxyapatite can successfully be used to tailor the density and mechanical properties of the final porous structures.

Keywords

Hydroxyapatite, urea, porous structure, sintering, mechanical properties, compressive strength, microhardness

Date received: 10 February 2015; accepted: 27 May 2015

Introduction

Hydroxyapatite (HA) has found wide application as a ceramic biomaterial due to its high biocompatibility and similarity in chemical composition with bone tissue.[1,2] Literature reports about fabrication of porous hydroxyapatite structures for bone repair and augmentation[3,4,5] with emphasis on the relevance of the size of the pores obtained in the final product for bone ingrowth.[6] In vivo research confirmed the importance of porous structure of the biomaterial used on the bone ingrowth[7] and studies revealed that macropores larger than 100 μm are needed to effectively host the cellular and extracellular components of bone and pores larger than 200 μm are effective in osteoconduction.[8]

Different methods[9,10] have been proposed and applied for the production of porous hydroxyapatite structures such as indirect solid free form fabrication,[11,12] gel casting,[13] and combination of gel-casting and polymer sponge.[14] However, among those methods incorporation of porogen particles draws particular attention due to the simplicity and economics of the procedure.[15,16]

Chang et al. reported that osteoconductivity initiates starting from a pore size of 50 μm and reaches its optimum value at a pore size of 300 μm.[17] On the other hand, Kuhne et al.[18] found out that osteoconductivity in HA with 500 μm pore size was greater than in HA with a pore size of 200 μm. However, obviously larger pores would negatively effect the

[1]Department of Mechanical Engineering, Mersin University, Yenisehir, Mersin, Turkey
[2]Department of Mechatronic Systems Engineering, Turkish-German University, Beykoz, Istanbul, Turkey
[3]SECTORCert GmbH, Buro Campus Deutz Siegburger Strasse 229c, Cologne, Germany
[4]Department of Mechanical Engineering, Bogazici University, Bebek, Istanbul, Turkey

Corresponding author:
Onder Albayrak, Department of Mechanical Engineering, Mersin University, Yenisehir 33343, Mersin, Turkey.
Email: albayrakonder@mersin.edu.tr

mechanical characteristics of HA. Therefore, selection of the pore size is a trade off between osteoconductivity and mechanical properties and solely depends on the particular application. Control of the mechanical properties is necessary while increasing the pore size of HA. Therefore, this work aims to determine the effect of pores larger than 600 μm on the mechanical properties of HA.

In this study, pelleted samples produced using HA powder with and without prior calcination were prepared with urea addition of 25 and 50 wt% along with control samples without any urea. Obtained samples were sintered at 1100 °C and 1200 °C for 2 h. Phase constitution, phase stability, densification, and mechanical properties of the samples were investigated in order to determine the effects of the calcination of the HA powder, the amount of urea added and the sintering temperature.

Materials and methods

In this study, commercially obtained HA powders (Alfa Aesar, 36731, calcium phosphate tribasic 34–40 % Ca, $Ca_{10}(OH)_2(PO_4)_6$) were used as matrix material. In order to investigate the effect of calcination on both the mechanical properties of the final product and the thermal stability of HA, half of the HA powders were calcined at 900 °C for 2 h whereas the other half was used as is (Figure 1). Commercially available spherical shaped urea particles (Igsas, Turkey) were sieved and urea particles of size 600–850 μm were used to form porous structure.

In order to investigate the effect of urea addition on the decomposition of HA and the mechanical properties of the final structure samples with two different urea amount (25 and 50 wt%) were prepared using both calcined and uncalcined HA. Similarly, samples were prepared using calcined and uncalcined HA without any urea addition.

A given amount of HA and urea particles were manually mixed together with a small amount of ethanol in a glass beaker for about 1 min to facilitate particles binding. Samples with HA/urea composition of 100/0, 75/25, and 50/50 wt% were uniaxially pressed (MSE, MP10, Turkey) into cylindrical specimen with 10 mm diameter and a h/d ratio larger than 1.2 in a stainless steel die applying a pressure of 100 MPa for 60 s. The prepared pellets were sintered at 1100 °C and 1200 °C for 2 h with a heating and cooling rate of 100 °C/h in air atmosphere.

The coding of the produced samples are given in Table 1 where "U" and "C" stand for uncalcined and calcined HA powders, respectively. Following 3 digits (100, 075, and 050) indicate the percentage of HA in the sample and the last 4 digits (0000, 1100, and 1200) show the sintering temperature such as 1100 °C and 1200 °C whereas 0000 indicates no sintering.

Phase stability and constitution of the used HA powders in uncalcined and calcined form before and after sintering were investigated by powder X-ray diffractometry (XRD) (Model SmartLab, Rigaku, Japan) to determine any possible HA decomposition. The XRD data were collected at a room temperature over the 2θ range of 10 °–70 ° at a step size of 0.02° and a count time of 1 s. Fourier transform infrared (FTIR) (Model FT-IR/FIR/NIR Spectrometer Frontier ATR, PerkinElmer, USA) analyses were conducted for the determination of the functional groups and structural changes. The measurements were carried out in the transmission mode in the mid-interface range (450–4000 cm^{-1}) at the resolution of 2 cm^{-1}. Sintered pellets were analyzed by field emission scanning electron microscopy (FESEM) (Zeiss, Supra 55, Germany) to determine the pore morphology and the sinterability of the samples.

Densities of the samples prior and after sintering were compared based on the dimensional and weight changes. The porosity of the samples after sintering stage was calculated by the formula $P = (1 - \rho/\rho_{th}) \times 100$, where ρ and ρ_{th} are the density of the samples and its corresponding theoretical density of 3.16 g/cm^3,[19] respectively.

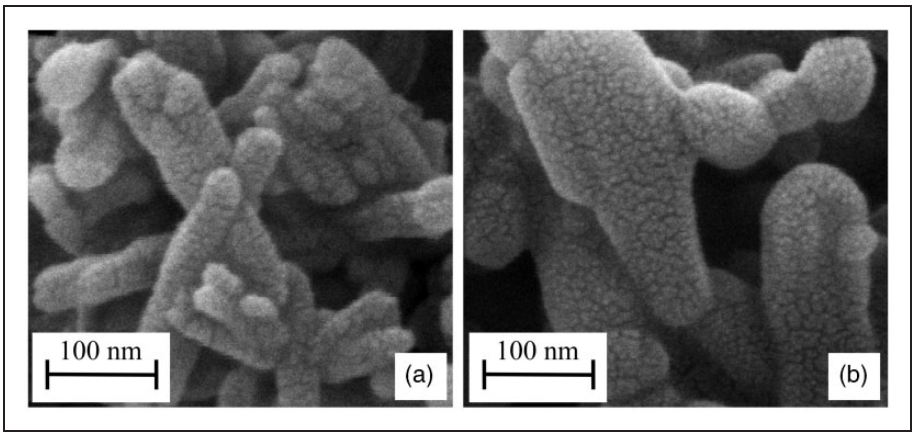

Figure 1. SEM images of HA powder in its as-received form and after calcination at 900°C for 2 h.

Table 1. Coding of the samples produced.

(w/w) % of HA/Urea	100/0			75/25			50/50		
Sintering Temp. (°C)	N/A	1100	1200	N/A	1100	1200	N/A	1100	1200
Uncalcined HA	U100-0000	U100-1100	U100-1200	U075-0000	U075-1100	U075-1200	U050-0000	U050-1100	U050-1200
Calcined HA	C100-0000	C100-1100	C100-1200	C075-0000	C075-1100	C075-1200	C050-0000	C050-1100	C050-1200

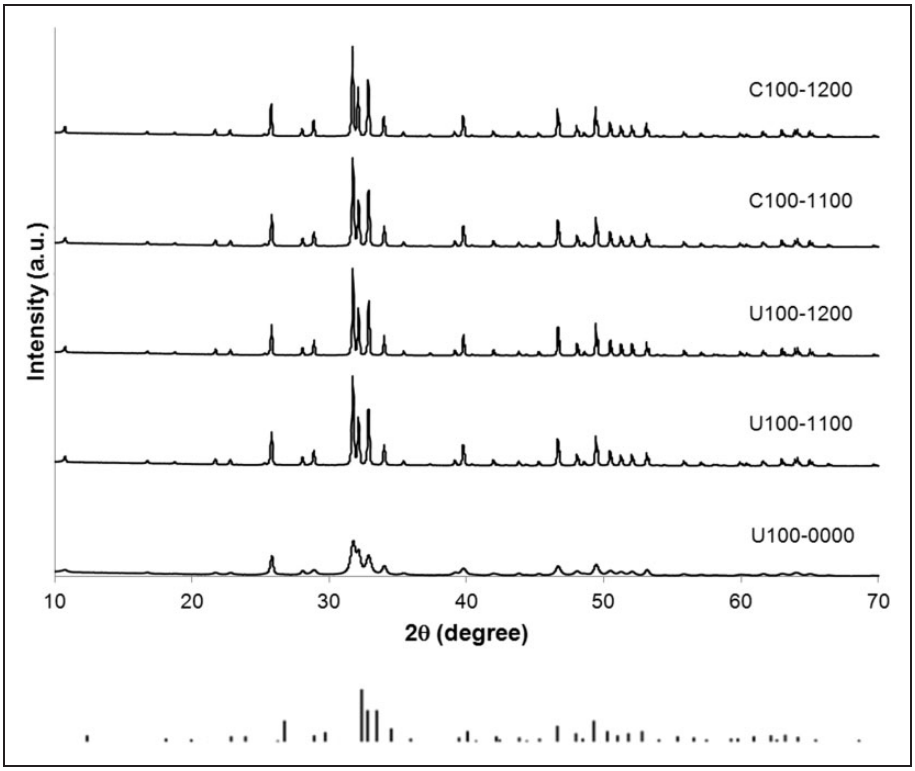

Figure 2. XRD spectra of HA powder in its as-received form (U100-0000) and in uncalcined and calcined states sintered at 1100°C and 1200°C compared to HA (JCPDS 86-0740).

In order to determine the effect of the calcination state on the hardness of the samples, Vickers microhardness measurements were conducted on sintered pellets without urea addition sintered at 1100 °C and 1200 °C with 200 g for 15 s after grinding-polishing. Five samples were used for each parameter set with five measurements on each sample.

Compression test was carried out on at least five samples in each group with a universal testing machine (Model Z100, Zwick, Germany) using a 10 kN load cell and a cross-head speed of 5.0 mm/min to determine the effects of calcinations, amount of urea added and sintering temperature on the compressive strength of the final products.

Results and discussions

In order to determine the effect of heat treatment on the phase stability of the powders XRD analysis was conducted and the results of the HA sample in its as-received state, uncalcined and calcined states, and sintered at 1100 °C and 1200 °C are presented in Figure 2. As seen in this figure, there are no apparent peaks other than HA as compared to HA (JCPDS 86-0740). Observation of the spectra revealed that the crystallization of the samples heat treated either in form of calcination or sintering was improved in comparison to the sample in its as-received form.

The FTIR spectra of the samples mentioned above and presented in Figure 2 are shown in Figure 3. HA-related characteristic PO_4^{3-} υ_4 bending bands around 567 and 602 cm^{-1}, PO_4^{3-} υ_1 band at 962 cm^{-1} and PO_4^{3-} υ_3 vibration bands around 1011 and 1093 cm^{-1} are visible in the IR spectra of HA (Figure 3) in its as-received form and after being heat treated at 1100 °C and 1200 °C.[20] The weak sharp peak at around 632 cm^{-1} which is the libration band originating from OH^- in the apatite is the characteristic band of HA.[20] With the application of thermal treatment in form of either calcination or

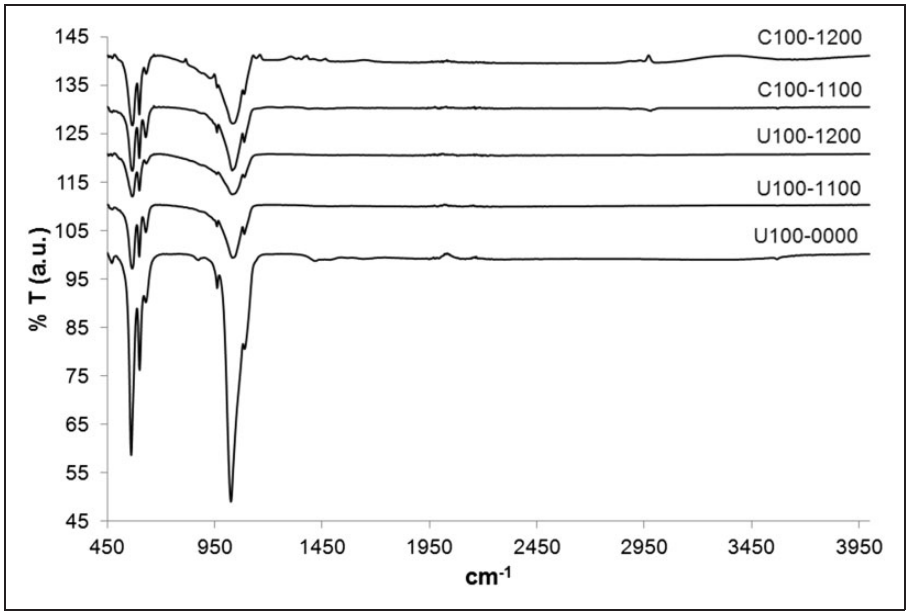

Figure 3. FTIR spectra of HA powder in its as-received form (U100-0000) and the U100 and C100 samples heat treated at 1100 °C and 1200 °C.

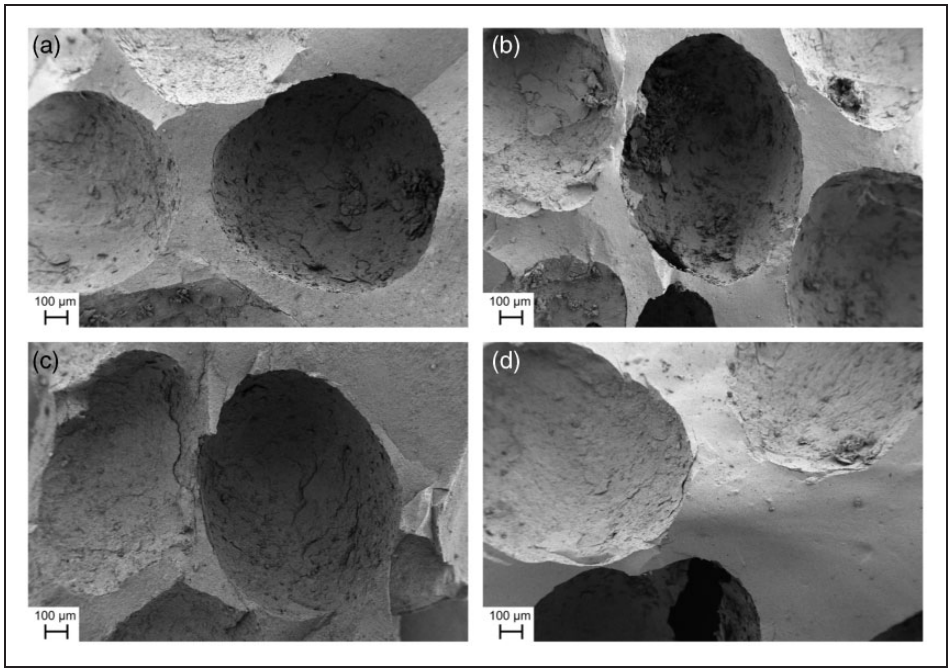

Figure 4. SEM images visualizing pore size and morphology in the samples prepared using: (a) UHA and 25 wt% urea, 1100 °C; (b) UHA and 25 wt% urea, 1200 °C; (c) CHA and 25 wt% urea, 1100 °C; (d) CHA and 25 wt% urea, 1200 °C.

sintering these peaks become weaker and broader. PO_4^{3-} and OH^- groups in FTIR spectra may be the evidence of the HA and so these FTIR graphs are in agreement with XRD observations.

SEM images were investigated to determine the pore morphology of the pellets (Figure 4). The pores are nearly spherical and distributed homogenously. Apparently, calcination of the HA used to prepare the pellets has no significant effect on the pore formation and morphology. Since pore size and pore morphology is independent of the amount of urea incorporated only SEM images of the pellet samples with 25 wt% urea are given in Figure 4.

SEM images (Figure 5) of the samples sintered at 1100 °C and 1200 °C revealed that increasing sintering temperature leads to better sinterability of the prepared pellets for a given amount of urea incorporated.

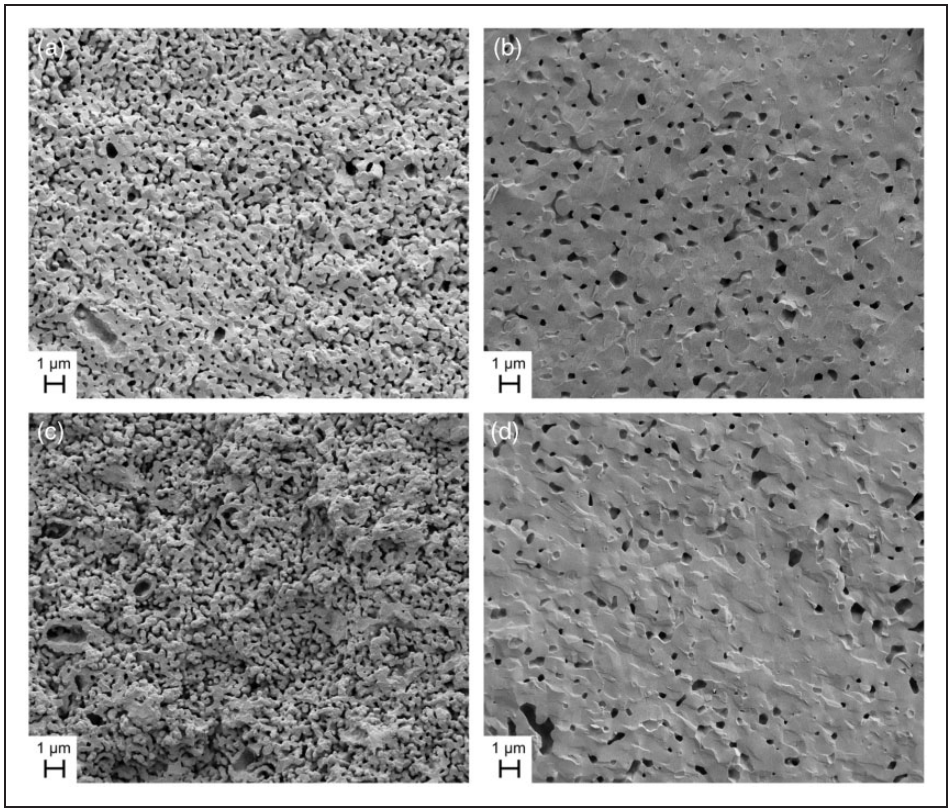

Figure 5. SEM images of the sintered samples prepared using uncalcined (UHA) and calcined (CHA) HA with different urea compositions: (a) UHA and 25 wt% urea, 1100 °C; (b) UHA and 25 wt% urea, 1200 °C; (c) CHA and 25 wt% urea, 1100 °C; (d) CHA and 25 wt% urea, 1200 °C.

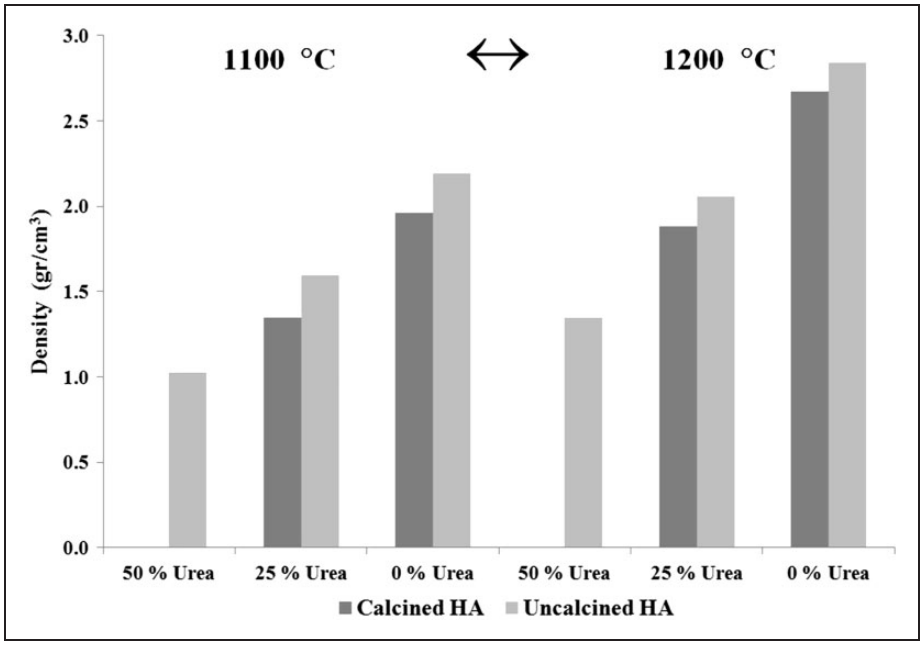

Figure 6. Densities of the samples sintered at 1100°C and 1200°C prepared using calcined and uncalcined HA powders with different urea content.

Densities of the prepared pellets were measured in order to determine the effect of urea addition on the densification behavior of the samples. Density measurements of the samples with varying urea content reveal that density decreases with increasing urea amount (Figure 6). Density increases with increasing sintering temperature related to the enhanced state of sintering at elevated temperatures.

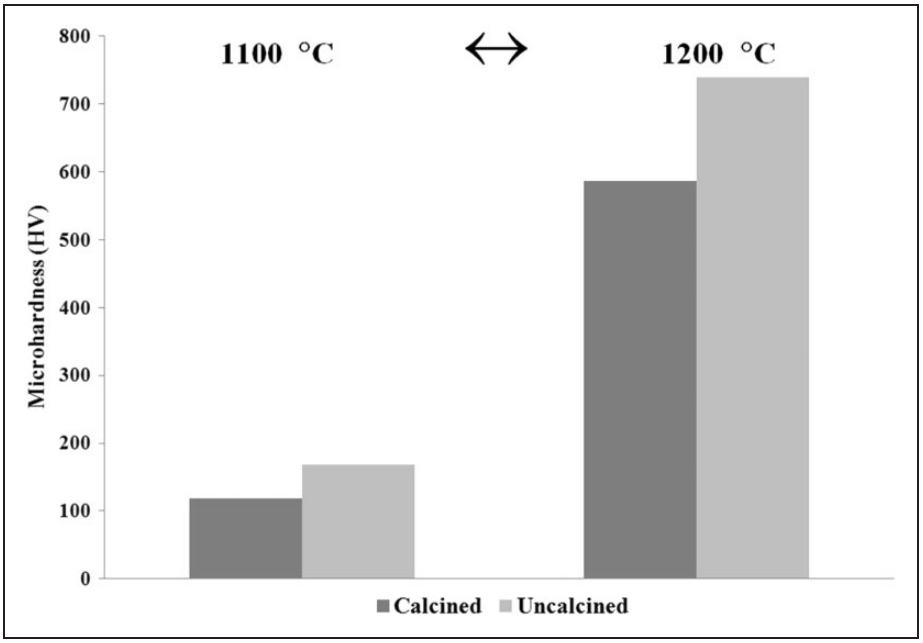

Figure 7. Microhardness values of the samples prepared with calcined and uncalcined HA and sintered at 1100 °C and 1200 °C.

Table 2. Porosities of the samples sintered at 1100 °C and 1200 °C prepared using calcined and uncalcined HA powders with different urea content.

Sintering temp. (°C)	1100			1200		
(w/w) % of HA/Urea	50/50	75/25	100/0	50/50	75/25	100/0
Calcined	N/A	57.41	37.78	N/A	40.36	15.51
Uncalcined	67.44	49.37	30.59	57.29	34.75	9.97

Important to note is the effect of prior calcination on the final density of the samples. Calcination seems to have a negative effect, in form of a slight decrease in density, on the densification behavior of the samples.

Similarly, the effect of the calcination is also apparent in the microhardness measurements of the samples where samples prepared with uncalcined HA have higher microhardness values than the samples prepared with calcined HA (Figure 7). Increasing the sintering temperature from 1100 °C to 1200 °C has a similar effect both for the samples prepared using uncalcined and calcined samples, namely microhardness increases by more than four times for both types of samples.

Samples prepared with uncalcined HA show better sinterability compared to samples prepared with calcined HA regardless of the sintering temperature and the amount of urea used, as observed by the percent porosities of the samples (Table 2). This may be attributable to the fact that the calcination process results in nodular-like particles increasing the particle size[21,22] and decreasing the surface area of the HA powder particles,[23] which effect the sinterability of the powder compact negatively. The SEM images of the uncalcined and calcined samples indicate an increase in particle size and change in aspect ratio (Figure 1) which is aggreement with the literature. Samples prepared with uncalcined HA powders might possess higher sinterability which in turn increases the compressive strength and the microhardness.

There is a significant difference in the density change for the samples (Figure 6) prepared using pure UHA and CHA and sintered at 1100 °C, which corresponds to a significant difference of the compressive strengths of the samples (Figure 8). With increasing sintering temperatures the difference of the compressive strengths of the pure UHA and CHA samples diminishes with the decreasing difference of the density changes of the samples.

In accordance with the SEM images presented in Figure 5, compression tests conducted on the pelleted samples sintered at 1100 °C and 1200 °C revealed that the compressive strength of the samples increase with increasing sintering temperature regardless of the calcination state of the HA powders and the urea content. Important to note is the effect of the prior calcination of the HA powders. Samples prepared with uncalcined HA powders have significantly higher compressive strengths at different sintering temperatures for different urea content than their counterparts prepared with calcined HA powders.

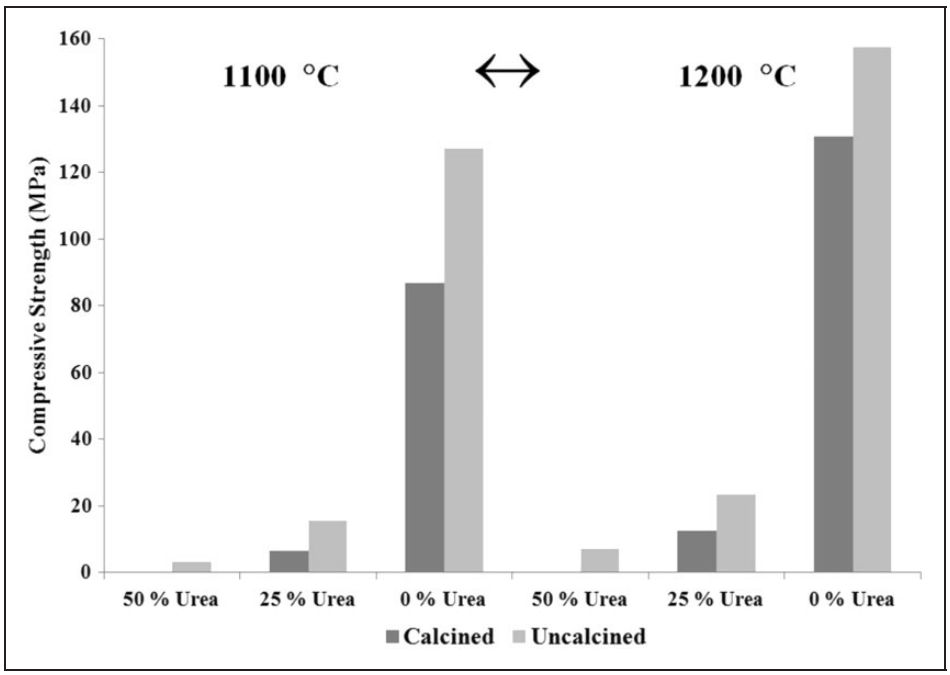

Figure 8. Compressive strengths of the samples sintered at 1100°C and 1200°C prepared using calcined and uncalcined HA powders with different urea content.

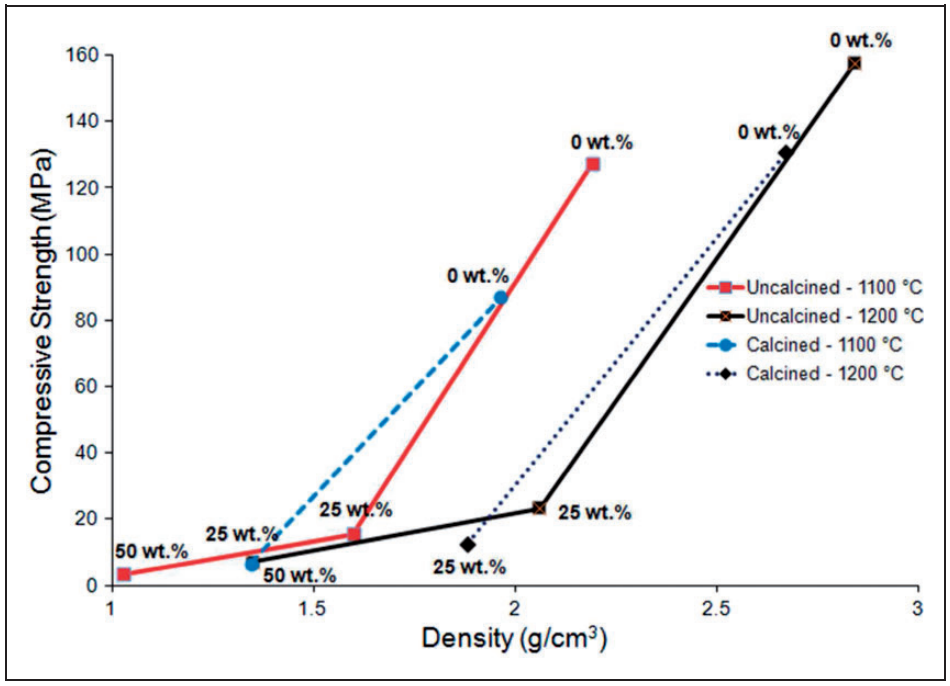

Figure 9. Compressive strength vs. density of the samples prepared using uncalcined and calcined HA powders with different urea concentration and sintered at 1100°C and 1200°C.

There is a direct relationship between the density and the compressive strength and microhardness of the prepared samples (Figures 9 and 10). Compressive strength increases as the densification is improved with the increasing temperature and use of uncalcined powder instead of calcined powder. Similarly, microhardness values of samples prepared with uncalcined powders are higher than those of the

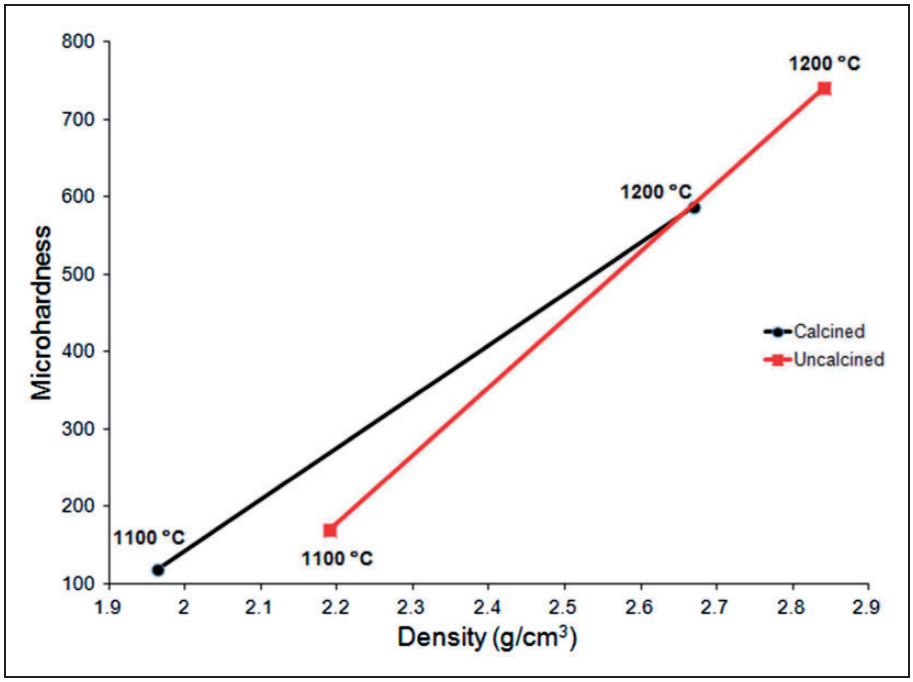

Figure 10. Microhardness vs. density of the samples prepared using uncalcined and calcined HA powders and sintered at 1100 °C and 1200 °C.

samples prepared with calcined powders and were observed to increase with the temperature as a result of the improved densification (Figure 10).

Conclusions

- Compressive strength and microhardness of HA increases with increasing sintering temperature regardless of the calcination state of the powder.
- Calcination negatively effects the densification and decreases the sinterability of HA further decreasing the compressive strength and microhardness. This negative effect is thought to be related to the increasing particle size due to calcination. Hence, similar compressive strengths may be attained at lower sintering temperatures by using uncalcined instead of calcined HA powder.
- Urea incorporation was found to be a successful method to produce porous HA structures. In order to increase porosity the amount of urea added can be increased which further leads to a decrease in compressive strength. However, this decrease in compressive strength can partially be compensated with the use of uncalcined HA powder. Hence, uncalcined HA is a good candidate to produce porous structures with smaller loss of compressive strength.

Acknowledgement

Authors would like to thank to "Mersin University Advanced Technology, Training, Research and Application Center" (MEITAM) for opportunity of using the SEM, XRD, and FTIR equipments.

Declaration of conflicting interests

The author(s) declared no potential conflicts of interest with respect to the research, authorship, and/or publication of this article.

Funding

The author(s) disclosed receipt of the following financial support for the research, authorship, and/or publication of this article: This work was supported in part by the Mersin University Scientific Research Projects (grant number: BAP-MUH F MM (OA) 2010-5A).

References

1. Hench LL. Biomaterials: A forecast for the future. *Biomaterials* 1998; 19: 1419–1423.
2. Albayrak O and Altintas S. Production of tricalcium phosphate / titanium dioxide coating surface on titanium substrates. *J Mater Sci Technol* 2010; 26: 1006–1010.
3. Ioku K, Somiya S and Yoshimura M. Dense/porous layered apatite ceramics prepared by HIP post-sintering. *J Mater Sci Lett* 1989; 8: 1203–1204.
4. Fabbri M, Celotti GC and Ravaglioli A. Hydroxyapatite-based porous aggregates: Physico-chemical nature, structure, texture and architecture. *Biomaterials* 1995; 16: 225–228.
5. Liu DM. Fabrication of hydroxyapatite with controlled porosity. *J Mater Sci Mater Med* 1997; 8: 227–232.
6. Ohashi H, Therin M, Meunier A, et al. The effect of drilling parameters on bone. III. The response to porous hydroxyapatite implants. *J Mater Sci Mater Med* 1994; 5: 237–241.

7. Dalcusi G and Passuti N. Effect of macroporosity for osseous substitution of calcium phosphate ceramic. *J Biomed Mater Res* 1990; 11: 86–87.
8. Hulbert SF, Morrison SJ and Klawitter JJ. Compatibility of porous ceramics with soft tissue; application to tracheal prostheses. *J Biomed Mater Res* 1971; 2: 269–279.
9. Li SH, de Wijn JR, Layrolle P, et al. Novel method to manufacture porous hydroxyapatite bt dual mixing. *J Am Ceram Soc* 2003; 86: 65–72.
10. Vargas S, Estevez M, Hernandez A, et al. Hydroxyapatite based hybrid dental materials with controlled porosity and improved tribological and mechanical properties. *Mater Res Innov* 2013; 17: 154–160.
11. Schek RM, Taboas JM, Segvich SJ, et al. Engineered osteochondral grafts using biphasic composite solid free-form fabricated scaffolds. *Tissue Eng* 2004; 10: 1376–1385.
12. Taboas JM, Maddox RD, Krebsbach PH, et al. Indirect solid free form fabrication of local and global porous, biomimetic and composite 3D polymer-ceramic scaffolds. *Biomaterials* 2003; 24: 181–194.
13. Sepulveda P, Ortega FS, Innocentini MDM, et al. Properties of highly porous hydroxyapatite obtained by the gelcasting of foams. *J Am Ceram Soc* 2000; 83: 3021–3024.
14. Ramay HR and Zhang M. Biphasic calcium phosphate nanocomposite porous scaffolds for load-bearing bone tissue engineering. *Biomaterials* 2004; 25: 5171–5180.
15. Zhang HG and Zhu Q. Preparation of porous hydroxyapatite with interconnected pore architecture. *J Mater Sci Mater Med* 2007; 18: 1825–1829.
16. Tsuruga E, Takita H, Itoh H, et al. Pore size of porous hydroxyapatite as the cell-substratum controls BMP-induced osteogenesis. *J Biochem* 1997; 121: 317–324.
17. Chang BS, Lee CK, Hong KS, et al. Osteoconduction at porous hydroxyapatite with various pore configurations. *Biomaterials* 2000; 21: 1291–1298.
18. Kuhne JH, Bartl R, Frisch B, et al. Bone formation in coralline hydroxyapatite. *Acta Orthop Scand* 1994; 65: 246–252.
19. Park JB and Lakes RS. *Biomaterials: An introduction*. 2nd ed. New York: Plenum Press, 1992.
20. Ye H, Liu XY and Hong H. Characterization of sintered titanium/hydroxyapatite biocomposite using FTIR spectroscopy. *J Mater Sci Mater Med* 2009; 20: 843–850.
21. Albayrak O, Oncel C, Tefek M, et al. Effects of calcination on electrophoretic deposition of naturally derived and chemically synthesized hydroxyapatite. *Rev Adv Mater Sci* 2007; 15: 10–15.
22. Ipekoglu M and Altintas S. Silver substituted nanosized calcium deficient hydroxyapatite. *Mater Technol* 2010; 25: 295–301.
23. Tan CY, Tolouei R, Ramesh S, et al. Calcination effects on the sinterability of hydroxyapatite bioceramics. In: *IFMBE Proceedings BIOMED 2011 '5th Kuala Lumpur international conference on biomedical engineering*, Kuala Lumpur, Malaysia, 2011, vol. 35, pp.51–54.